Chambers, edited by R. P. Shutt (Academic, New York, 1967), Vol. I, p. 159.
[14]S. Praestein, ANL/HEP Report No. 7140, 1971 (unpublished).
[15]R. Bock, CERN Report No. DD/EXP/62/10, 1962 (unpublished).
[16]Particle Data Group, Rev. Mod. Phys. 43, S1 (1971).
[17]W. Heitler, *The Quantum Theory of Radiation* (Clarendon, London, 1957).
[18]J. W. Motz, H. A. Olsen, and H. W. Koch, Rev. Mod. Phys. 41, 581 (1969).
[19]H. A. Bethe and J. Ashkin, in *Experimental Nuclear Physics*, edited by E. Segrè (Wiley, New York, 1960), Vol. I, p. 328.
[20]G. Bozoki, E. Fenyves, T. Gemesy, E. Gombosi, S. Krasznovszky, E. Nagy, N. P. Bogachev, Yu. A. Budagov, V. B. Vinogradov, A. G. Volodko, V. P. Dzhelepov, V. G. Ivanov, V. S. Kladnitsky, S. V. Klimenko, Yu. F. Lomakin, Yu. P. Merekov, I. Patočka, V. B. Fliagin, and P. V. Shlyapnikov, Phys. Letters 28B, 360 (1968).
[21]M. E. Binkley, D. W. Carpenter, J. R. Elliot, L. R. Fortney, E. C. Fowler, J. P. Golson, J. E. Kronenfeld, C. M. Rose, T. R. Snow, and W. M. Yeager, Phys. Rev. D 4, 3250 (1971).
[22]Tai Ho Tan, Phys. Rev. Letters 23, 102 (1969).
[23]C. Mayeur, P. Van Binst, G. Wilquet, V. B. Fliagine, J. G. Guy, W. L. Knight, S. N. Tovey, R. M. Dowd, M. Govan, A. J. Sanders, J. Schneps, and G. Wolsky, Phys. Letters 33B, 441 (1970).
[24]Jae Kwan Kim, Phys. Rev. Letters 27, 356 (1971).

PHYSICAL REVIEW D VOLUME 7, NUMBER 5 1 MARCH 1973

Final States with Three Charged Particles and a Visible Λ from K^-d Interactions at 4.5 GeV/c*

A. C. Ammann,† D. D. Carmony, A. F. Garfinkel, L. J. Gutay, and D. H. Miller
Physics Department, Purdue University, Lafayette, Indiana 47907

and

W. L. Yen
Physics Department, Indiana University-Purdue University at Indianapolis, Indianapolis, Indiana 46205
(Received 2 June 1972)

This report concerns itself with the study of four- or five-body final states produced by the interaction of 4.48-GeV/c K^- mesons on neutrons. The data result from a 372 000-picture exposure in the Argonne National Laboratory 30-in. deuterium-filled bubble chamber. The reactions studied include (1) $K^-n \to \Lambda\pi^+\pi^-\pi^-$, (2) $K^-n \to \Sigma^0\pi^+\pi^-\pi^-$, (3) $K^-n \to \Lambda\pi^+\pi^-\pi^-\pi^0$, (4) $K^-n \to \Lambda\pi^+\pi^-\pi^-$MM, (5) $K^-n \to \Lambda\pi^-K^+K^-$, and (6) $K^-n \to \Lambda\pi^-K^0_LK^0_S$, where all the Λ particles decayed visibly. Evidence is presented for the existence of the $\Sigma(1640)$ whose mass and width are 1642 ± 12 MeV/c^2 and 55 ± 24 MeV/c^2, respectively. The branching ratios are found to be consistent with an octet assignment. The A_2 data are presented and are compatible with $J^{PC} = 2^{++}$. In addition, the productions of ρ^0, ω, and ϕ^0 are discussed in conjunction with simultaneous $\Sigma^-(1385)$ production and the results are compared with quark-model predictions.

I. INTRODUCTION

The primary purpose of this experiment was to study the interaction of K^- mesons with neutrons. To this end, 372 000 exposures were made at the deuterium-filled MURA 30-in. bubble chamber at Argonne National Laboratory using a 4.48-GeV/c K^- beam. Almost all the data analyzed here consist of four- and five-particle final states containing a visible Λ decay. Four- and five-particle final states containing a visible $\overline{K}^0$ decay[1] and two- and three-particle final states containing a visible neutral decay[2,3] have been studied elsewhere.

Analysis of the data is divided into three sections. The existence and branching ratios of hyperon resonances in the 1.6-GeV/c^2 mass region is investigated under the topic of baryon resonances. Included under meson resonances is a study of the controversial A_2 region of the three-pion mass spectrum. The angular distributions and cross sections of the quasi-two-body reactions resulting in baryon–vector-meson resonance production are compared with predictions of the quark model in the last section.

II. EXPERIMENTAL DETAILS

The film was scanned for events of the types three- or four-prong plus vee and one- or two-prong plus two vees. In the case of even-prong events it was demanded that one of the positive particles (the spectator) had a range of less than 15 cm. All events of these topologies were mea-

sured on three scanning and measuring projectors (SMP) on-line to an IBM-360/40-44 system which provided geometric reconstruction (TVGP). The kinematic fitting was performed off-line on the IBM-360/44 using the Berkeley program SQUAW.

Out of the approximately 8000 events with an associated vee, 4474 were unambiguously identified as Λ' s and 2978 as $\overline{K}^0$'s. In addition, 532 vees were regarded as ambiguous since both mass interpretations fitted the production vertex with at least 0.1% probability and the positive decay track had a momentum greater than 1.2 GeV/c so that identification on the basis of ionization was impossible. The distribution (not shown) of the cosine of the angle between the $\overline{K}^0$ and the outgoing π^+ in the $\overline{K}^0$ rest frame is, as required by parity conservation, flat whereas the corresponding distribution (Fig. 1) for the Λ's has a depression in it which is nicely filled by the ambiguous events. We, therefore, included the ambiguous events in the Λ sample.

For the Λ sample, the following five hypotheses were considered:

$$K^-d \to p_s\pi^+\pi^-\pi^-\Lambda\,, \tag{1}$$

$$K^-d \to p_s\pi^+\pi^-\pi^-\Sigma^0,\quad \Sigma^0 \to \Lambda\gamma\,, \tag{2}$$

$$K^-d \to p_s\pi^+\pi^-\pi^-\Lambda\pi^0\,, \tag{3}$$

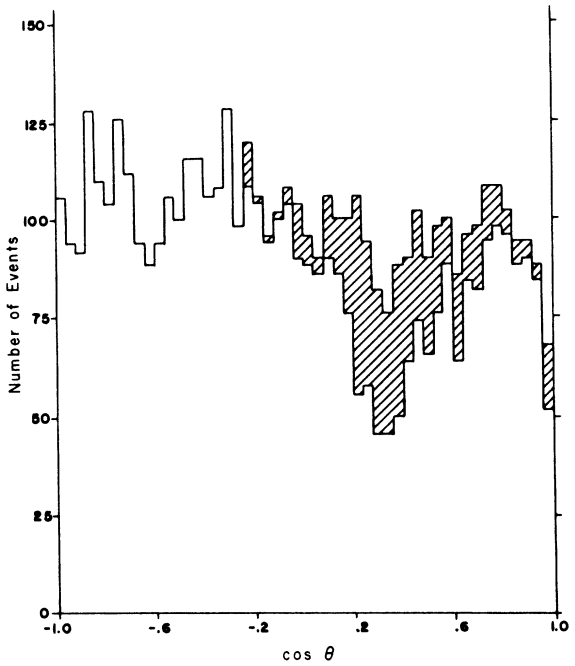

FIG. 1. Distribution in cosθ, where θ is the angle between the vee direction and the decay proton as measured in the vee rest frame for the vee's selected to be Λ. The shaded portion corresponds to the ambiguous vee events.

$$K^-d \to p_s\pi^+\pi^-\pi^-\Lambda\mathrm{MM}\,, \tag{4}$$

$$K^-d \to p_s K^+K^-\pi^-\Lambda\,, \tag{5}$$

where p_s is the spectator proton, an MM is the missing mass. In order for a given hypotheses to be considered acceptable, it was necessary that the confidence level for that hypothesis be greater than 1%. This cutoff provides a unique assignment for events of reaction (5). It also resolves most of the ambiguities between reactions (1) and (3), but leaves the ambiguities between reactions (1) and (2) and between reactions (2) and (3) essentially unchanged.

We used the following scheme[4] to assign events for reactions (1), (2), and (3). Let C_Λ, C_Σ, and C_π, be the confidence levels of the fits for reactions (1), (2), and (3), respectively. An event was assigned to reaction (1) if $C_\Lambda > 1.3C_\Sigma$ and $C_\Lambda > C_\pi$. An event was assigned to reaction (2) if $C_\Sigma > 1.4C_\Lambda$ and $C_\Sigma > 2.5C_\pi$. Finally, an event was assigned to reaction (3) if $C_\pi > 1.2C_\Lambda$ and $C_\pi > C_\Sigma$.

The following tests of our selection criteria were made: The momenta of the decay Λ's in the Σ^0 rest frames were examined and found to lie predominantly in the plane containing the beam and Σ^0 momenta for the events accepted as "true Λ" events. For the "true Σ^0" events they were found to be isotropically distributed. When an event was accepted as a true Λ, true Σ^0, or true π^0 event, the hyperon missing mass M_H for the reaction $K^-n \to \pi^+\pi^-\pi^-M_H$ was calculated. The M_H distribution showed separate peaks at the Λ and Σ^0 masses for Λ and Σ^0 events, respectively. For π^0 events, the M_H distribution showed the characteristic $\Sigma(1385)$ structure on top of a $\Lambda\pi^0$ invariant-mass phase space.

There were 295 events remaining ambiguous. We excluded those events from the following analysis and made a small correction to the cross section for the lost events.

The number of events assigned to each reaction is given in Table I together with the corresponding cross sections. The cross-section calculation was corrected for beam purity, scanning efficiency, Glauber screening effect, Λ branching ratio, losses due to failures in the reconstruction program, and detection efficiency for the Λ.

III. BARYON RESONANCES

The most prominent baryon structure in the data is the well-known $\Sigma(1385)$ which is seen in all the Λ-pion mass combinations. A second isospin-1 enhancement is seen in these mass spectra centered around 1.64 GeV/c^2. This enhancement, which was the subject of an earlier letter,[5] will

TABLE I. Cross sections.

Reaction Final states	Cross section (μb)	Reaction Final states	Cross section (μb)
$K^-n \to \Lambda\pi^+\pi^-\pi^-$	171 ± 9 (497 events)	A_2 production	
$\Sigma^0\pi^+\pi^-\pi^-$	78 ± 7 (242 events)	$K^-n \to \Lambda(\pi^+\pi^-\pi^-)$	12 ± 3
$\Lambda\pi^+\pi^-\pi^-\pi^0$	548 ± 14 (1781 events)	$\Sigma^0(\pi^+\pi^-\pi^-)$	5 ± 2
$\Lambda\pi^+\pi^-\pi^-$MM	451 ± 20 (1558 events)		
$\Lambda\pi^-K^+K^-$ / $K_L^0K_S^0$	117 ± 7 (189 events) (118 events)	ω production	
		$K^-n \to \Lambda\pi^-(\pi^+\pi^-\pi^0)$	73 ± 6
$\Sigma(1385)$ production		ϕ production	
$K^-n \to (\Lambda\pi^+)\pi^-\pi^-$	37 ± 4	$K^-n \to \Lambda\pi^-$ { K^+K^- / $K_L^0K_S^0$ / $\pi^+\pi^-\pi^0$ }	43 ± 4
$(\Lambda\pi^+)\pi^-\pi^-\pi^0$	58 ± 5		
$(\Lambda\pi^+)\pi^-\pi^-$MM	35 ± 5	R region	
$(\Lambda\pi^0)\pi^+\pi^-\pi^-$	25 ± 4	$K^-n \to \Lambda(\pi^+\pi^-\pi^-\pi^0)$	20 ± 3
$(\Lambda\pi^-)K^+K^-$ / $K_L^0K_S^0$	36 ± 5	Quasi-two-body reactions	
$(\Lambda\pi^-)\pi^+\pi^-\pi^0$	100 ± 7	$K^-n \to \Sigma^-(1385)\phi$	18 ± 3
$(\Lambda\pi^-)\pi^+\pi^-$MM	74 ± 7	$\Sigma^-(1385)\omega$	10 ± 2
$\Sigma(1640)$ production		$\Sigma^-(1385)\rho^0$	5 ± 3
$K^-n \to (\Lambda\pi^+)\pi^-\pi^-$	7 ± 3		
$(\Lambda\pi^-)\pi^+\pi^-$	7 ± 3		
ρ production			
$K^-n \to \Lambda\pi^-\pi^-(\pi^+\pi^0)$	22 ± 3		
$\Lambda\pi^-(\pi^+\pi^-)$	30 ± 4		
$\Sigma^0\pi^-(\pi^+\pi^-)$	16 ± 3		
$\Lambda\pi^-\pi^0(\pi^+\pi^-)$	59 ± 6		
$\Lambda\pi^-(\pi^+\pi^-)$MM	26 ± 5		
$\Lambda\pi^+\pi^-(\pi^0\pi^-)$	28 ± 4		
$\Lambda(\pi^+\pi^-)(\pi^0\pi^-)$	<6		

henceforth be referred to as the $\Sigma(1640)$ and evidence is presented for its interpretation as the previously reported $\Sigma(1620)$.[6,7] The production cross sections associated with $\Sigma(1385)$ or $\Sigma(1640)$ are presented in Table I.

A. Mass Fitting

The $\Sigma(1640)$ is seen predominantly in the final state $\Lambda\pi^+\pi^-\pi^-$, in both possible charge states (Fig. 2). This is the only final state used in fitting for mass and width, not only because of the relative prominence of the $\Sigma(1640)$, but also because other final states involve lower-constraint kinematic fits and hence poorer resolution. The mass resolution for the $\Sigma(1640)$ in the final state considered is 12 ± 3 MeV/c^2.

In the mass fitting, simple Breit-Wigner functions of the following form

$$B(m) \propto \frac{\frac{1}{2}\Gamma^2}{(m_R - m)^2 + \frac{1}{4}\Gamma^2}$$

were used to represent the $\Sigma(1385)$ and $\Sigma(1640)$ resonances. Γ is the full width at half-maximum, m_R is the resonance mass, and m is the invariant mass. These curves were added incoherently to a smooth background function of the form

$$P(m) \propto (m - m_L)(m_U - m)e^{a(m - m_c)},$$

where m_L and m_U are the lower and higher limits of m and m_c is the average of m_L and m_U. In addition to the background parameter a, the mass, width and amount of both resonances were permitted to vary. The fit is shown in Fig. 2 and the fitted parameters are presented in Table II.

B. Production Mechanism

Figure 3 shows $|t - t_0|$ versus $M(\Lambda\pi)$, where t is the four-momentum transfer squared from the neutron to the $\Lambda\pi$ combination and $|t_0|$ is the minimum kinematically allowed momentum transfer squared. Both the $\Sigma(1385)$ and $\Sigma(1640)$ seem to be produced predominantly at small $|t - t_0|$. Although the four-momentum-transfer distributions are consistent with meson exchange and K or $K^*(890)$ exchange may be important for the $\Lambda\pi^-$ case, substantial resonant $\Lambda\pi^+$ is also seen, and therefore the possibility of a cascade-type mechanism was investigated. Plots of $M^2(\Lambda\pi)$

versus $M^2(\Lambda\pi^+\pi^-)$ in Fig. 4 shows no strong clustering of $\Sigma(1385)$ or $\Sigma(1640)$ events in any band of $\Lambda\pi^+\pi^-$ mass. The $\Sigma^+(1640)$ may show some tendency to be produced for $M^2(\Lambda\pi^+\pi^-)$ around 7 $(\mathrm{GeV}/c^2)^2$. In order to search for a reaction of the form

$$\Sigma^* \to \Sigma(1640)\pi,$$

$$\Sigma(1640) \to \Lambda\pi,$$

the $\Sigma(1640)$ was defined as

$$1.61 < M(\Lambda\pi) < 1.67\ \mathrm{GeV}/c^2,$$

and the following weighted plot was constructed. Labeling the negative pions, π_a^- and π_b^-, each $\Lambda\pi^+\pi^-$ combination was plotted the number of times shown below in Table III. [An asterisk in the $\Lambda\pi$ columns indicates the presence of a $\Sigma(1640)$.]

The plot is shown in the shaded portion of Fig. 5(a), the outer histogram showing each $\Lambda\pi^+\pi^-$ combination plotted twice. There appears to be a clear enhancement in the $\Lambda\pi^+\pi^-$ spectrum just below 2.6 GeV/c^2 for events having a $\Sigma(1640)$ combination. Identical plots (not shown) for control regions on either side of $\Sigma(1640)$ do not show this structure. The signal persists undiminished when events containing a $\Sigma(1385)$, ρ^0, or A_2 are removed. A hyperon resonance is known in this region, the $\Sigma(2595)$ (Ref. 8); however, so far it has only been seen to decay to $N\bar{K}$. If this reaction indeed occurs, it accounts for fewer than 25% of the $\Sigma(1640)$ events and could not be the only production mechanism. Events having $2.52 < M(\Lambda\pi^+\pi^-) < 2.68$ do have an enhancement of the $\Sigma(1640)$ in both charge states. In Fig. 5(b) each $\Lambda\pi$ mass combination in the 1640 region has been plotted if no A_2, ρ, or $\Sigma(1385)$ combination is present. The solid curve is a smoothed representation of the $\Lambda\pi^+\pi^-$ background obtained by selecting $\Lambda\pi$ masses in bands above $(1.67\text{–}1.73\ \mathrm{GeV}/c^2)$ and below $(1.55\text{–}1.61\ \mathrm{GeV}/c^2)$ the $\Sigma(1640)$. The

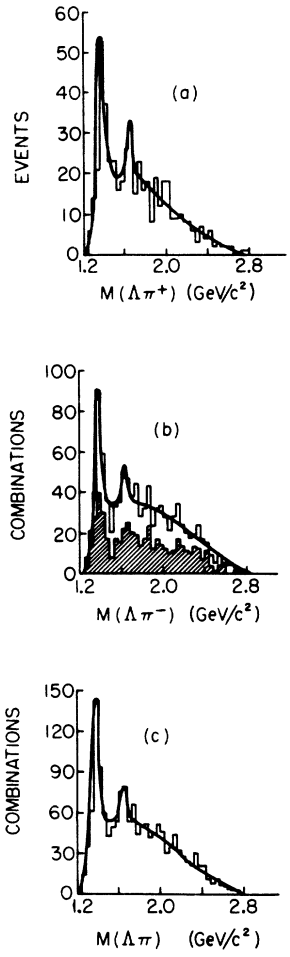

FIG. 2. $\Lambda\pi$ mass spectra in 40-MeV/c^2 bins for the reaction $K^-n \to \Lambda\pi^+\pi^-\pi^-$: (a) $\Lambda\pi^+$, (b) $\Lambda\pi^-$, two combinations per event, (c) $\Lambda\pi$, i.e., sum of (a) and (b), containing three combinations per event. The smooth curves represent simple Breit-Wigner fits to the data. The shaded portion in (b) is the combination having lower $|t - t_0|$ from n to $\Lambda\pi^-$.

TABLE II. Fitted parameters of $\Lambda\pi$ mass spectra.

	$\Lambda\pi^+$	$\Lambda\pi^-$	$\Lambda\pi$	$\Lambda\pi$ and unfolding the mass resolution of 12 ± 3 MeV/c^2
a	-2.05 ± 0.20	-1.22 ± 0.14	-1.42 ± 0.10	
		For $\Sigma(1385)$		
M (GeV/c^2)	1.380 ± 0.005	1.380 ± 0.004	1.380 ± 0.003	1.380 ± 0.005
Γ (GeV/c^2)	0.060 ± 0.016	0.062 ± 0.010	0.063 ± 0.010	0.061 ± 0.010
A (%)	19.8 ± 3.4	17.8 ± 2.0		
		For $\Sigma(1640)$		
M (GeV/c^2)	1.650 ± 0.006	1.631 ± 0.009	1.642 ± 0.010	1.642 ± 0.012
Γ (GeV/c^2)	0.018 ± 0.012	0.046 ± 0.025	0.059 ± 0.023	0.055 ± 0.024
A (%)	3.4 ± 1.8	3.6 ± 1.0		

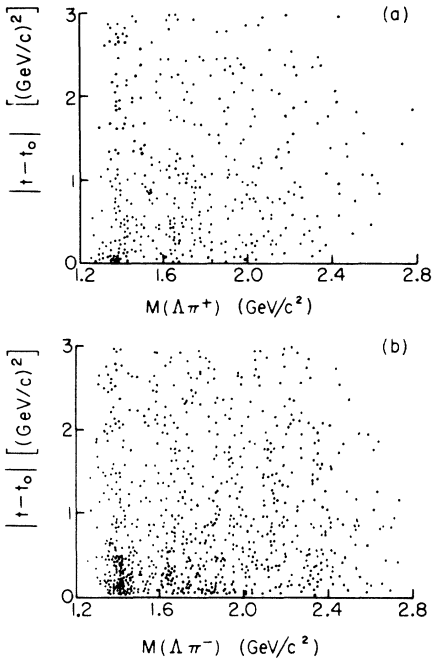

FIG. 3. Chew-Low plots for $K^-n \to \Lambda\pi^+\pi^-\pi^-$: (a) $\Lambda\pi^+$ system, (b) $\Lambda\pi^-$ system.

curve is normalized to the total number of events in the plot. The enhancement just below 2.6 GeV/c^2 is seen to persist.

In order to eliminate the possibility of the $\Sigma(1640)$ being a kinematic reflection of other resonances in this channel, all known structures were removed and the remaining events inspected. Figure 6 shows all three $\Lambda\pi$ combinations, the shaded portion representing those remaining after removal of known resonances. It can be seen that the $\Sigma(1640)$ signal is reduced, but still present. Removal of the A_2 produces no loss of signal but there is some slight tendency to share particles among the $\Sigma(1385)$ and the $\Sigma(1640)$. Most of the signal loss occurs upon removal of ρ^0 events. Among these, the biggest loss is in the negative charge state. This is expected since a ρ^0 may be produced simultaneously with a $\Sigma^-(1640)$ and thus removal of the ρ^0 events may remove some legitimate $\Sigma^-(1640)$ events even though we see no evidence of strong quasi-two-body $\Sigma^-(1640)$ ρ production. Inspecting a plot of $M(\Lambda\pi_a^-)$ against $M(\pi^+\pi_a^-)$ shows no particular tendency for events to lie in the $\Sigma^-(1640)\rho^0$ intersection and thus gives no indication of strong particle sharing.

C. Branching Ratios and Assignment

Because of the small number of events, errors associated with the branching ratios of the $\Sigma(1640)$ are quite large. Despite these large errors the

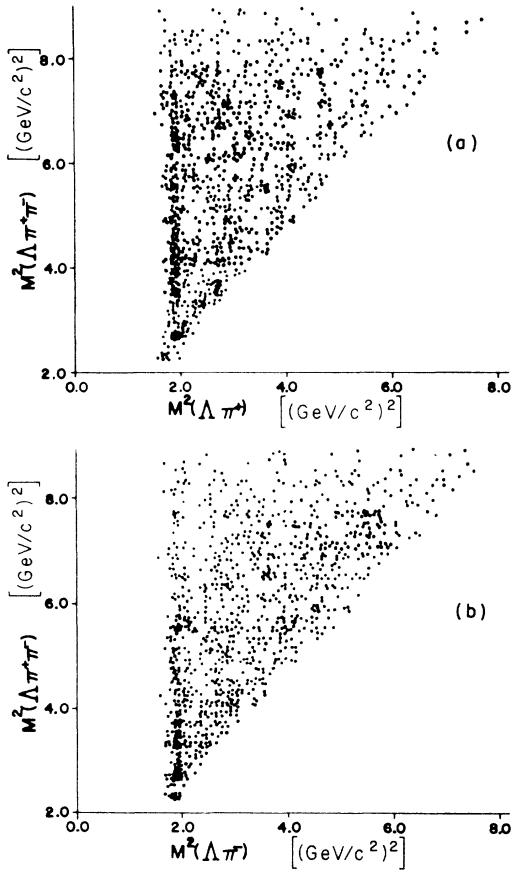

FIG. 4. Scatter plot of $M^2(\Lambda\pi)$ versus $M^2(\Lambda\pi^+\pi^-)$ for $K^-n \to \Lambda\pi^+\pi^-\pi^-$: (a) for $\Lambda\pi^+$, (b) for $\Lambda\pi^-$.

identification of the $\Sigma(1640)$ with certain known resonances, in particular the $\Sigma(1660)$ resonances,[9] can be ruled out.

Figure 7(a) shows the $\Sigma^0\pi$ mass spectrum containing three combinations per event. There is little or no evidence for the $\Sigma(1640)$. Accounting for charged Σ events which are not included, an upper limit on the $\Sigma\pi$ to $\Lambda\pi$ branching ratio can

TABLE III. Weights used to test $(\Lambda\pi\pi) \to \Sigma(1640)\pi$. An asterisk in the $\Lambda\pi$ columns indicates the presence of a $\Sigma(1640)$.

$\Lambda\pi^+$	$\Lambda\pi_a^-$	$\Lambda\pi_b^-$	Weight of $\Lambda\pi^+\pi_a^-$	Weight of $\Lambda\pi^+\pi_b^-$
			0	0
		*	0	4
	*		4	0
	*	*	2	2
*			2	2
*		*	1	3
*	*		3	1
*	*	*	2	2

be estimated as

$$\frac{\Sigma(1640)\to\Sigma\pi}{\Sigma(1640)\to\Lambda\pi}<1.0$$

at a 95% confidence level.

A similar situation exists in Fig. 7(b), the $\Sigma^0\pi^+\pi^-$ mass spectrum, which has two combinations per event. There is no evidence for an enhancement at 1.64 GeV/c^2.

The reaction $K^-n\to p\bar{K}^0\pi^-\pi^-$, which has been reported in Ref. 1, can be used to measure the branching ratio to KN where N is a nucleon. The $p\bar{K}^0$ mass distribution [Fig. 8(a)] shows marginal evidence of the process $\Sigma(1640)\to\bar{K}N$. A branching ratio was estimated to be

$$\frac{\Sigma(1640)\to\bar{K}N}{\Sigma(1640)\to\Lambda\pi}=0.4\pm0.4\,.$$

A natural question to ask is whether the $\Sigma(1640)$ is actually one of the two $\Sigma(1660)$ states resolved by Eberhard *et al.*[9] They found that their lower-mass component which we denote by $\Sigma_L(1660)$, decays predominantly to $\Sigma\pi\pi$ with the $\Sigma\pi\pi$ spectrum peaking at 1651 MeV/c^2. The other component which we denote by $\Sigma_H(1660)$ was found to decay roughly twice as often to $\Sigma\pi$ as to $\Sigma\pi\pi$, with the $\Sigma\pi$ spectrum peaking at 1667 MeV/c^2. The $\Sigma_L(1660)$ was said to show a measurable decay to $\Lambda\pi$ with the branching ratio

$$\frac{\Sigma_L^+(1660)\to\Lambda\pi^+}{\Sigma_L^+(1660)\to\Sigma^\pm\pi^\mp\pi^+}=0.4\pm0.13\,,$$

where $\Sigma^\pm\pi^\mp$ is predominantly a decay of the $\Lambda(1405)$. Events in our experiment corresponding to the reaction $K^-n\to\pi^+\pi^-\pi^-$ MM were examined (where MM decayed to a visible Λ plus possible neutrals) for evidence of the process

$$K^-n\to\Sigma^\pm(1640)\pi^\mp\pi^-,$$

$$\Sigma^\pm(1640)\to\Lambda(1405)\pi^\pm,$$

$$\Lambda(1405)\to\Sigma^0\pi^0.$$

In Fig. 8(b), events with $1.38<\mathrm{MM}<1.43$ GeV/c^2 were selected as possible $\Lambda(1405)$ and their (MM)π spectrum was plotted. No $\Sigma(1640)$ is apparent in the (MM)π spectrum. In view of the branching ratio quoted by Eberhard *et al.*, the $\Sigma(1640)$ must be different from the low-mass component $\Sigma_L(1660)$.

Eberhard *et al.* do not discuss the $\Lambda\pi$ branching ratio of the high-mass component $\Sigma_H(1660)$. One might argue that the high-mass component (~1667 MeV/c^2) is too far removed from 1640 MeV/c^2 for the states to be identical. While this is probably true, we would further argue that one can reasonably obtain the decay branching ratios of $\Sigma_H(1660)$ from the phase-shift results of Armenteros *et al.*[10] This is because the state detected in the phase-shift analysis has a very low branching fraction to $\Sigma\pi\pi$ and hence can contain only a

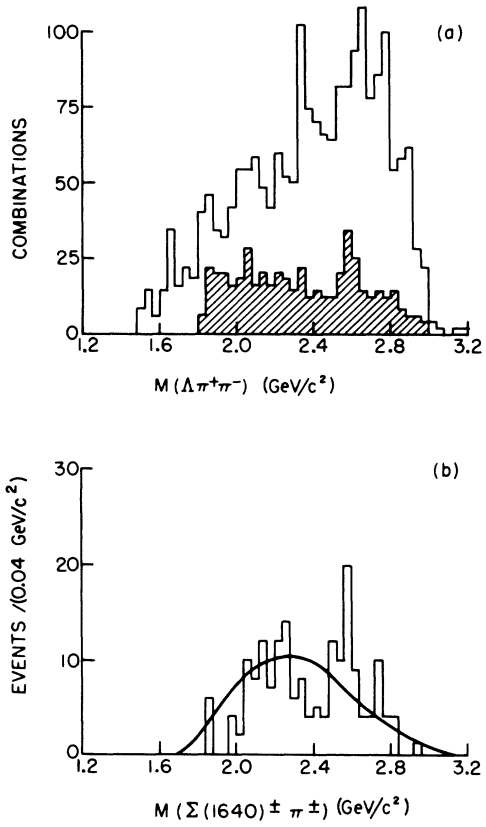

FIG. 5. (a) The $\Lambda\pi^+\pi^-$ effective mass in 40-MeV/c^2 bins for $K^-n\to\Lambda\pi^+\pi^-\pi^-$; the shaded portion shows the weighted plot (see text). (b) $\Sigma(1640)\pi$ effective mass; the curve is explained in the text.

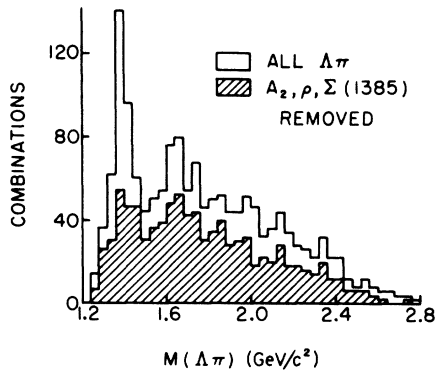

FIG. 6. $\Lambda\pi$ mass plot for $K^-n\to\Lambda\pi^+\pi^-\pi^-$. Each event has been plotted three times.

very small admixture of $\Sigma_L(1660)$. Hence we compare our value of less than 1.1 for the relative $\Sigma\pi/\Lambda\pi$ branching ratios of the $\Sigma(1640)$ with that of 1.7 found in Ref. 10. They seem to be in substantial disagreement. Hence the $\Sigma(1640)$ appears to be different from either of the $\Sigma(1660)$ states described in the literature.

One may conclude that the most probable interpretation of the $\Sigma(1640)$ is to associate it with the $\Sigma(1620)$ reported by Crennell *et al.*[6,7] The weighted average of our mass and width (with those of Crennell *et al.*[6,7]) are 1626 ± 7 and 66 ± 14 MeV/c^2, respectively. Those values lie closest to the mass and width of the P_{11} state of Ref. 10, making the $\Sigma(1640)$ an attractive candidate for a member of a second $\frac{1}{2}^+$ octet along with the P_{11} nucleon state at 1470 MeV/c.

Finally a search for the $\Sigma(1640)$ in other final states has produced negative results. Figure 9 shows the $\Lambda\pi$ mass for final states (3)–(5). Although there are clear $\Sigma(1385)$ signals, little evidence for a $\Sigma(1640)$ is seen.

IV. MESON RESONANCES

In this section several meson resonances are investigated. In addition, evidence of structure in the four-pion mass is presented. The production cross sections associated with ρ, A_2, ω, ϕ, or R are given in Table I.

A. ρ Meson

The ρ meson is seen most clearly in the final state $\Lambda\pi^+\pi^-\pi^-$. Figure 10 shows the $\pi^+\pi^-$ mass spectrum which contains two combinations per event. The shaded portion is the combination having lower $|t - t_0|$ from the K^- to the ρ^0. The smooth curve represents a fit to the data using the same background and resonance forms described in Sec. III A. Results of the fit are summarized in Table IV. The fitted width of 50 ± 21 MeV/c^2 differs sharply from the accepted world average value[11] of 125 ± 20 MeV/c^2. A similar effect has been observed in our one-prong plus V data of the same exposure.[2]

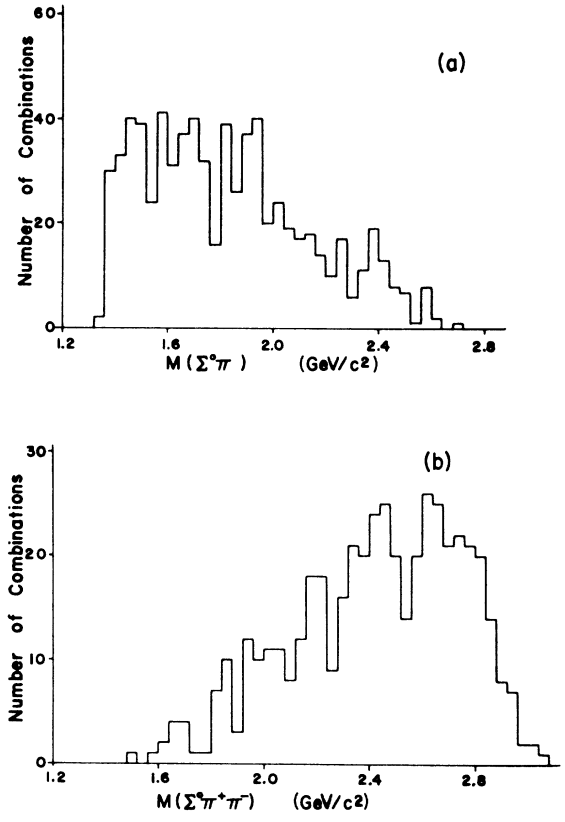

FIG. 7. Mass plots in 40-MeV/c^2 bins for $K^-n \to \Sigma^0\pi^+\pi^-\pi^-$: (a) $M(\Sigma^0\pi)$, three combinations per event; (b) $M(\Sigma^0\pi^+\pi^-)$, two combinations per event.

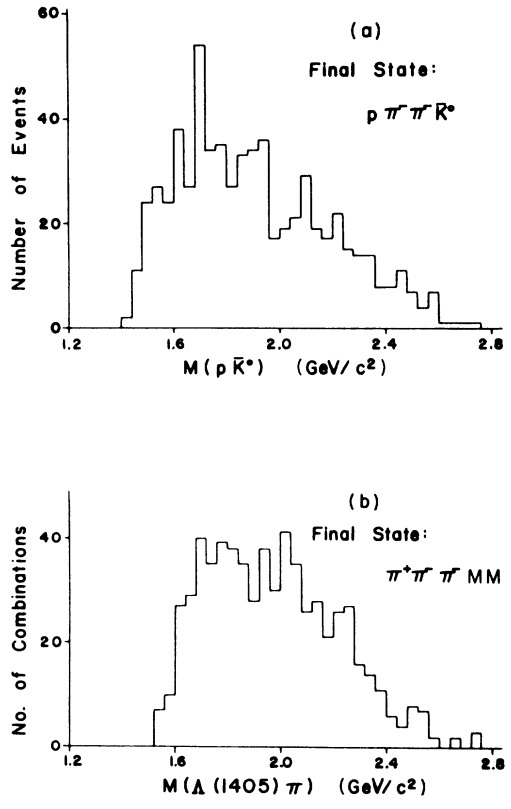

FIG. 8. Mass plots in 40-MeV/c^2 bins for (a) $M(p\bar{K}^0)$ from $K^-n \to p\pi^-\pi^-\bar{K}^0$, (b) $M(\Lambda(1405)\pi)$, $\Lambda(1405)$ is selected from $K^-n \to \pi^+\pi^-\pi^-$MM, with $1.38 < \text{MM} < 1.43$ GeV/c^2.

TABLE IV. Mass, width, and amount of meson resonances.

	Mass (GeV/c^2)	Width (GeV/c^2)	Amount (%)
ρ from reaction (1)	0.752 ± 0.007	0.050 ± 0.021	9.1 ± 2.6
A_2 from reaction (1)	1.336 ± 0.012	0.051 ± 0.040	8.0 ± 3.8
A_2 from reaction (2)	1.340 ± 0.014	0.120 ± 0.090	8.4 ± 4.2
ω	0.780	0.012	
ϕ	1.020 ± 0.005	0.005 ± 0.005	

In Fig. 11 the $M(\pi^+\pi^-)$ is plotted against the four-momentum transfer squared from the incident K^- to the dipion system. The clustering of events at low $|t-t_0|$ is suggestive of meson exchange, presumably the K or $K^*(890)$ mesons. The ρ^0 production mechanism is studied in more detail in conjunction with $\Sigma^-(1385)$ production in Sec. V.

The two-pion mass is shown for other final states in Fig. 12. A definite ρ^0 signal is seen in the final state $\Sigma^0\pi^+\pi^-\pi^-$ and again it appears to be very narrow. As before, the shaded portion represents the combination having lower $|t-t_0|$. The ρ does not appear as strong in the final state $\Lambda\pi^+\pi^-\pi^-\pi^0$, but five dipion combinations are plotted for each event in this case.

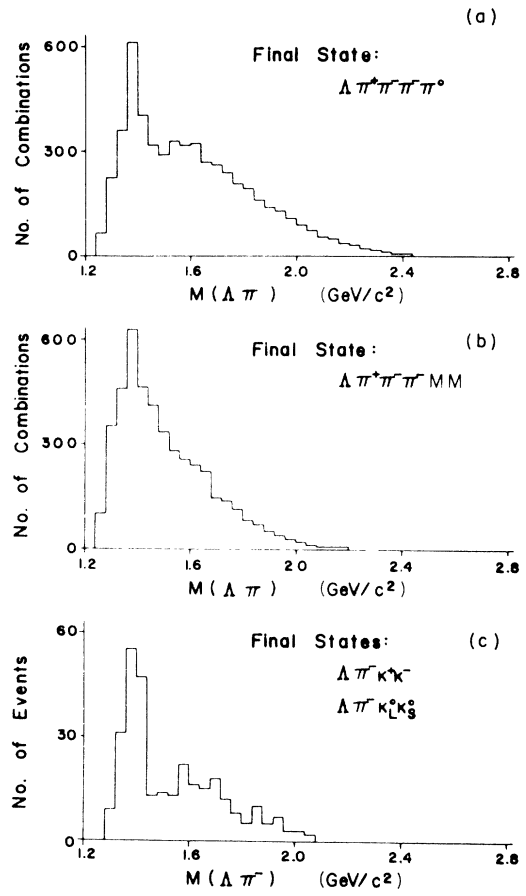

FIG. 9. The $\Lambda\pi$ effective mass in 40-MeV/c^2 bins: (a) $K^-n \to \Lambda\pi^+\pi^-\pi^-\pi^0$, (b) $K^-n \to \Lambda\pi^+\pi^-\pi^-$MM, (c) $K^-n \to \Lambda\pi^-K^+K^-$ and $K^-n \to \Lambda\pi^-K^0_L K^0_S$. Three combinations per event for both (a) and (b).

B. The A_2 Region

Enhancements in the three-pion mass spectrum (Fig. 13) are seen in reactions (1) and (2). The smooth curves in Fig. 13 represent fits to the data using the same background and resonance form described in Sec. IIIA. Results of the fit are summarized in Table IV. These enhancements occur at around 1.3 GeV/c^2, the region of the A_2 meson. As the properties of our A_2^- meson have already been reported elsewhere,[12] we shall only summarize the main results.

Since the first indications of the existence of the A_2 meson,[13] that object has inspired continual interest. Chung *et al.*[14] recognized quite early that the A_2 must have a $J^P = 2^+$ component (or 4^+, 6^+, ...) by their observation of the production reaction

$$\pi^- p \to A_2^- p,$$

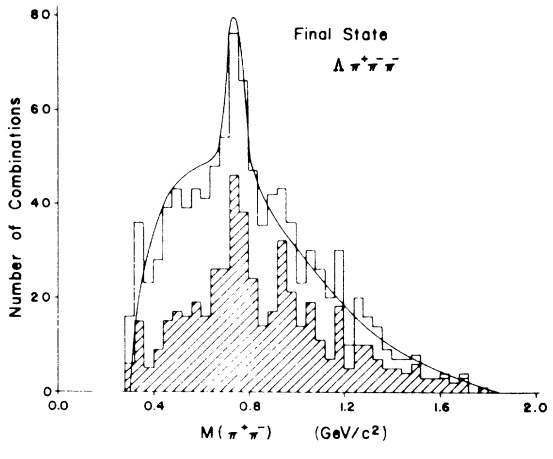

FIG. 10. $\pi^+\pi^-$ mass for $K^-n \to \Lambda\pi^+\pi^-\pi^-$ in 40-MeV/c^2 bins. The shaded portion is the combination having lower $|t-t_0|$ from the K^- to the ρ^0. The smooth curve represents a simple Breit-Wigner fit to the data.

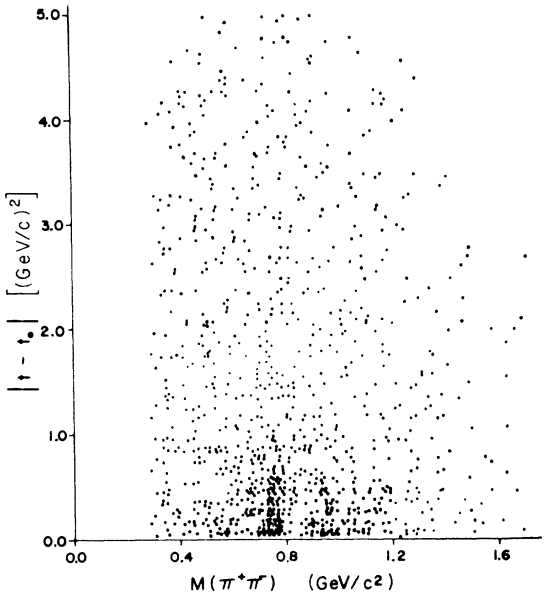

FIG. 11. The Chew-Low plot for the $\pi^+\pi^-$ system in the reaction $K^-n \to \Lambda\pi^+\pi^-\pi^-$.

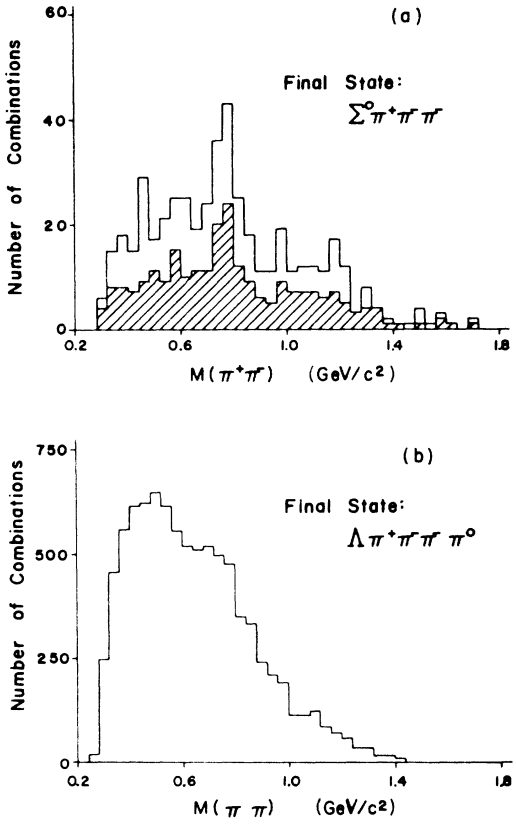

FIG. 12. The $\pi\pi$ mass plots in 40-MeV/c^2 bins for (a) $K^-n \to \Sigma^0\pi^+\pi^-\pi^-$, (b) $K^-n \to \Lambda\pi^+\pi^-\pi^-\pi^0$. All $\pi\pi$ combinations except $\pi^-\pi^-$ are plotted in both (a) and (b).

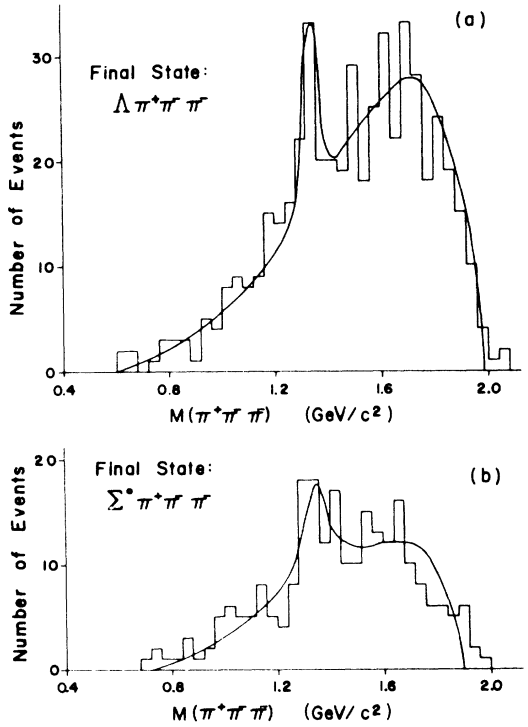

FIG. 13. The $\pi^+\pi^-\pi^-$ mass plots in 40-MeV/c^2 bins for (a) $K^-n \to \Lambda\pi^+\pi^-\pi^-$, (b) $K^-n \to \Sigma^0\pi^+\pi^-\pi^-$. The curves are fitted to the data using a Breit-Wigner form plus a smooth background described in Sec. III A of the text.

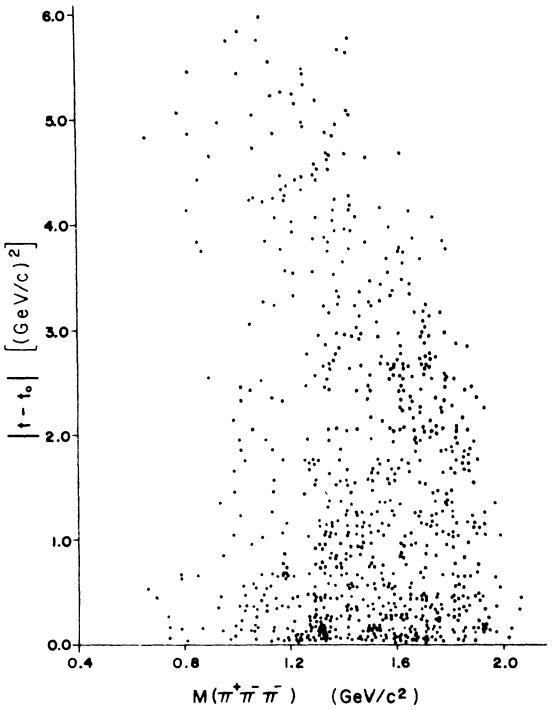

FIG. 14. Chew-Low plot for the $\pi^+\pi^-\pi^-$ system from $K^-n \to \Lambda\pi^+\pi^-\pi^-$ and $K^-n \to \Sigma^0\pi^+\pi^-\pi^-$.

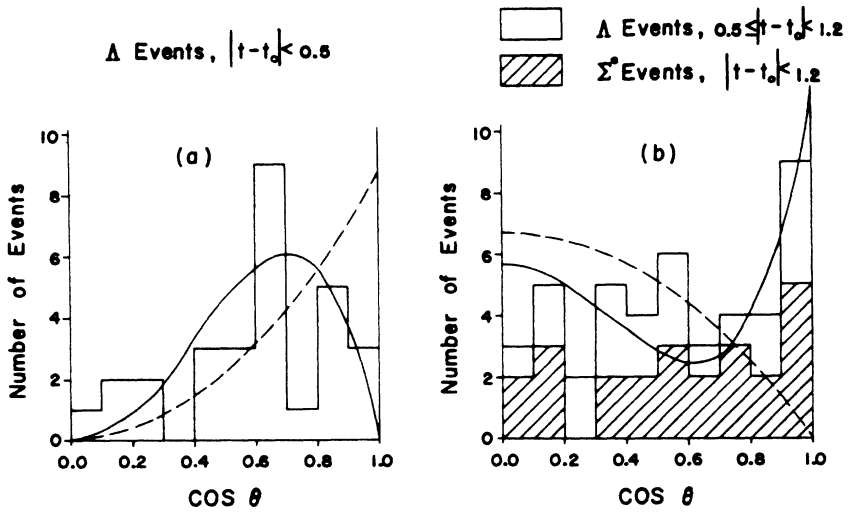

FIG. 15. Cosθ (the Jackson angle) distribution for events in the A_2 region: (a) $K^-n \to \Lambda\pi^+\pi^-\pi^-$, (b) $K^-n \to \Lambda\pi^+\pi^-\pi^-$ with $0.5 \leq |t-t_0| < 1.2$ (GeV/c)^2 and $K^-n \to \Sigma^0\pi^+\pi^-\pi^-$ with $|t-t_0| < 1.2$ (GeV/c)^2. The dashed curves show the expected distributions for mesons of J^P equal to 1^-. The solid curves are for mesons of J^P equal to 2^+.

with the subsequent decays

$$A_2^- \to K^-K^0$$

and

$$A_2^- \to \pi^-\pi^-\pi^+ .$$

Further analysis would be required[15] if the CERN missing-mass spectrometer group[16] observation of splitting of the A_2 is substantiated.

In a previous study of kaon-induced A_2 production, Crennell *et al.*[17] have analyzed the reaction $K^-n \to A_2^-\Lambda$ at an incident momentum of 3.9 GeV/c. They found a narrow peak at 1.289 GeV/c^2 having width less than or about 40 MeV/c^2. Although $J^P = 2^+$ is not ruled out for this $\rho\pi$ structure, they favor a spin-parity assignment of $J^P = 1^-$. Their A_2 has $I = 1$ and $C = +1$ which would imply difficulties for the simple quark model since a quark-antiquark pair cannot form a $J^{PC} = 1^{-+}$ state.

Our three-pion mass is plotted against the four-momentum transfer ($K^- \to \pi^+\pi^-\pi^-$) in Fig. 14. Events from reactions (1) and (2) are both plotted. Those events in the A_2 mass region [$1.28 < M(3\pi) < 1.38$ GeV/c^2] show a tendency to be produced at low $|t-t_0|$. This suggests that K and/or $K^*(890)$ may be exchanged. The ratio of coupling constants $g_{\Sigma KN}/g_{\Lambda KN}$ is known to be small.[18,19] Therefore, only $K^*(890)$ exchange can contribute appreciably to reaction (2). This assumption is supported by separate plots for the two reactions (not shown). A_2 events belonging to reaction (1) tend to cluster at low $|t-t_0|$ while A_2 events from reaction (2) show much weaker preference for the forward direction.

In order to study the spin and parity of the A_2 production in these reactions, the events were divided into two categories. The first category includes all reaction (1) events satisfying $|t-t_0| < 0.5$ (GeV/c)^2 which lie in the A_2 mass region. This sample is presumably rich in events produced primarily by K-meson exchange. All reaction (2) events satisfying $|t-t_0| < 1.2$ (GeV/c)^2 are included in the second category. The sample also contains events from reaction (1) satisfying $0.5 < |t-t_0| < 1.2$ (GeV/c)^2. $K^*(890)$ exchange should hopefully dominate these events.

Angular distributions for these two cases are shown in Fig. 15. The angle θ is the angle be-

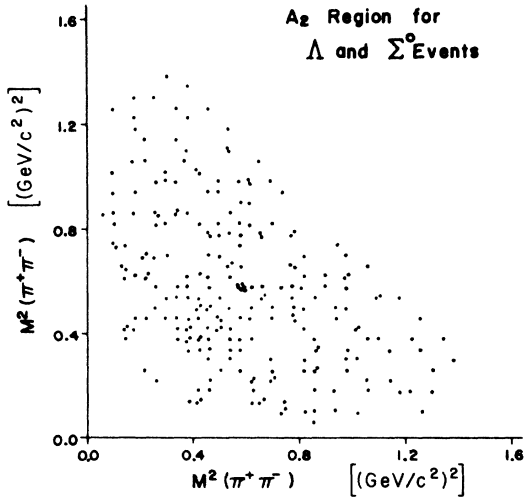

FIG. 16. The Dalitz plot for the A_2 region from $K^-n \to \Lambda\pi^+\pi^-\pi^-$ and $K^-n \to \Sigma^0\pi^+\pi^-\pi^-$.

tween the beam and the normal to the A_2 decay plane in the A_2 center-of-mass system. The normal is defined as the cross product of the three-momenta of the negative pions. Since the plots are folded about $\cos\theta = 0$, the sign is unimportant.

For pure K exchange, the probability distributions for the decay of 1^- and 2^+ mesons have the following form[20]:

$$P_{1^-}(\theta) \propto \cos^2\theta$$

and

$$P_{2^+}(\theta) \propto \cos^2\theta(1-\cos^2\theta),$$

respectively. For pure $K^*(890)$ exchange, they have the form

$$P_{1^-}(\theta) \propto (1-\cos^2\theta)$$

and

$$P_{2^+}(\theta) \propto (1-3\cos^2\theta+4\cos^4\theta).$$

These are the four curves shown in Fig. 15. Although background is difficult to estimate, the curves indicate that a J^P assignment of 2^+ is favored over 1^-. Had we not divided the Λ events into two momentum-transfer regions, our data, like the 3.9-GeV/c data, would seem to imply $J^P = 1^-$. Our analysis does not determine the J^P of the K^-n produced A_2, but does indicate compatibility with the accepted 2^+ value.

The A_2 seen in other experiments appears as an enhancement in the $\rho\pi$ mass spectrum. However, the dominant decay mode in this data is $A_2 \to \pi^+\pi^-\pi^-$. Defining the ρ^0 region as $0.70 < M(\pi^+\pi^-) < 0.82$ GeV/c^2 and forming the $\rho^0\pi^-$ combination yields only a small A_2 signal above background. Conversely, selecting A_2 events and plotting possible ρ^0 combinations shows essentially no relative ρ enhancement above that seen in the complete sample.[12] Thus our A_2 has the very strange property that while a $\rho^0\pi^-$ decay mode is not excluded, it is definitely small compared to the $\pi^+\pi^-\pi^-$ mode. It would be interesting to see if other K^-n experiments confirm this observation.

For a 2^+ object decaying into $\rho^0\pi^-$, the Dalitz plot (Fig. 16) in the A_2 region should show strong constructive interference at the intersection of the ρ^0 bands. Crennell *et al.*[17] find little evidence for such an effect and use this as a supporting argument for $J^P = 1^-$ assignment for their A_2. Since the $\rho^0\pi^-$ decay mode is apparently small in our data, it is difficult to observe if this interference exists.

C. The ω Meson

Figure 17 shows the $\pi^+\pi^-\pi^0$ mass spectrum from reaction (3), the shaded portion having the lower $|t-t_0|$ $(K^- \to \pi^+\pi^-\pi^0)$. Choosing the combination with the lower $|t-t_0|$ leaves the ω signal unreduced. Figure 18 displays $|t-t_0|$ against the neutral three-pion mass. The ω does seem to be pro-

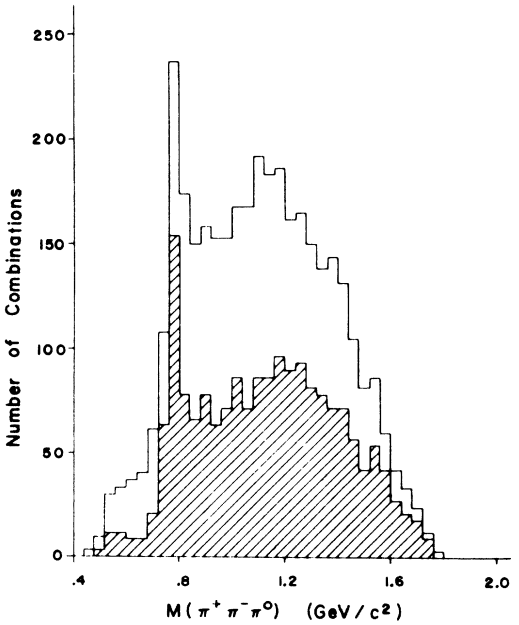

FIG. 17. $\pi^+\pi^-\pi^0$ mass spectrum from $K^-n \to \Lambda\pi^+\pi^-\pi^-\pi^0$. The shaded portion has the lower $|t-t_0|$ $(K^- \to \pi^+\pi^-\pi^0)$.

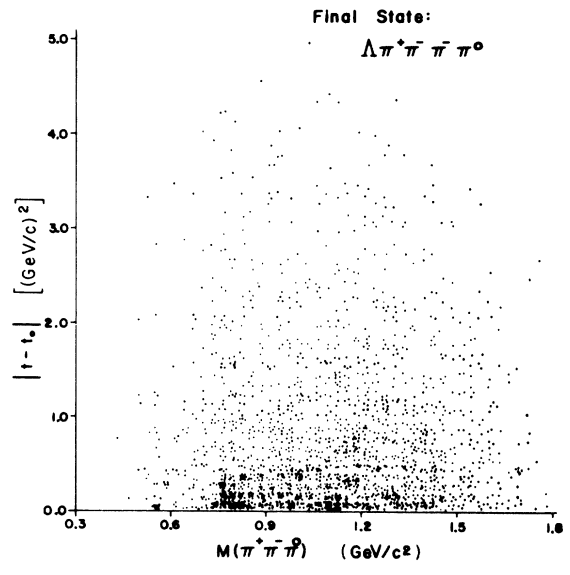

FIG. 18. The Chew-Low plot for the $\pi^+\pi^-\pi^0$ system from $K^-n \to \Lambda\pi^+\pi^-\pi^-\pi^0$.

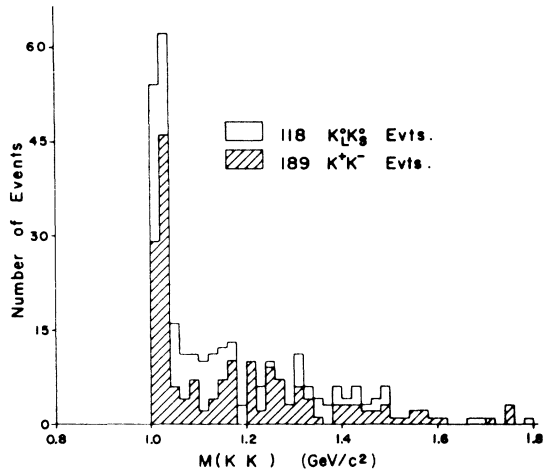

FIG. 19. The KK mass in 20-MeV/c^2 bins from $K^-n \to \Lambda\pi^- K^+ K^-$ and $K^-n \to \Lambda\pi^- K^0_S K^0_L$.

duced peripherally, as very few events lie above $|t - t_0| = 0.5$ (GeV/c)^2. The ω is studied further in Sec. V in conjunction with $\Sigma^-(1385)$ production.

D. The ϕ Meson

The ϕ meson is seen predominantly in two final states. Most of the events come from the reaction

$$K^-n \to \Lambda\pi^-\phi,$$

$$\phi \to K^+K^-.$$

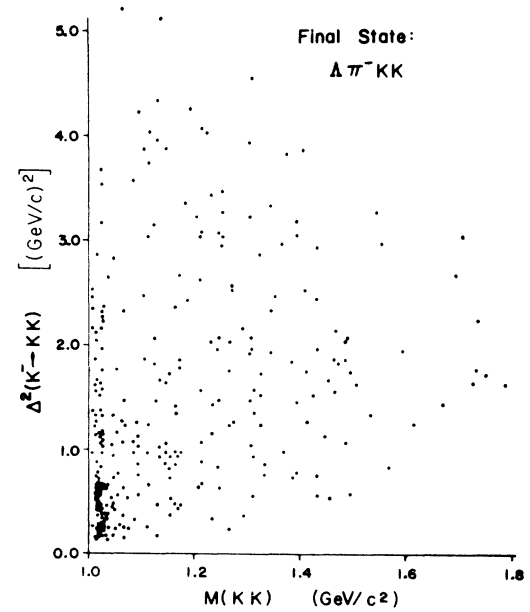

FIG. 20. The Chew-Low plot for the KK system from $K^-n \to \Lambda\pi^- K^+ K^-$ and $K^-n \to \Lambda\pi^- K^0_S K^0_L$.

The remaining events are taken from one- and two-prong plus two-vee topology, in particular the reaction

$$K^-n \to \Lambda\pi^-\phi,$$

$$\phi \to K^0_S K^0_L.$$

The KK mass is shown in Fig. 19 for events selected from both topologies. There are about 30 events in the ϕ band which decay to neutral kaons with the kaons subsequently decaying to $\pi^+\pi^-$. About 63 events decay to charged kaons. Taking account of the branching ratios of K^0_S, we find that

$$\frac{\phi \to K^0_S K^0_L}{\phi \to K^+K^-} = 0.76$$

in excellent agreement with the listed value in Ref. 11.

A Chew-Low plot (Fig. 20) for the combined sample shows that the ϕ tends to be produced peripherally. This will be investigated in Sec. V with regard to $\Sigma^-(1385)$ production.

There is no evidence for the reaction

$$K^-n \to \Lambda K^- K^*,$$

$$K^* \to K^+\pi^-$$

in these events. This is not unexpected since a one-particle-exchange model requires the ex-

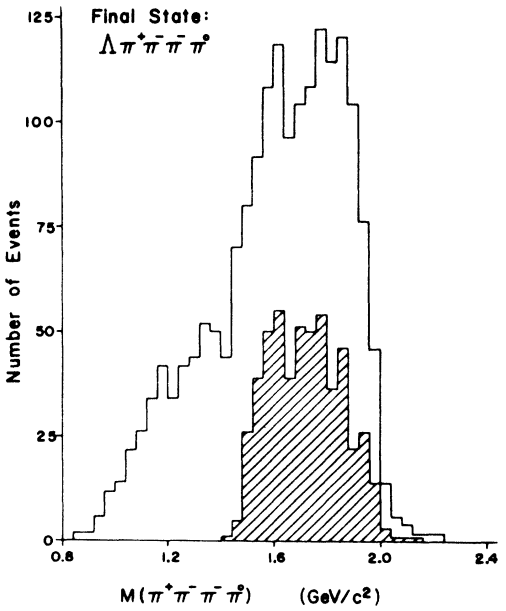

FIG. 21. The 4π mass distribution in 40-MeV/c^2 bins for $K^-n \to \Lambda\pi^+\pi^-\pi^-\pi^0$. The shaded portion represents those events for which an appropriate 3π combination may form an A_2.

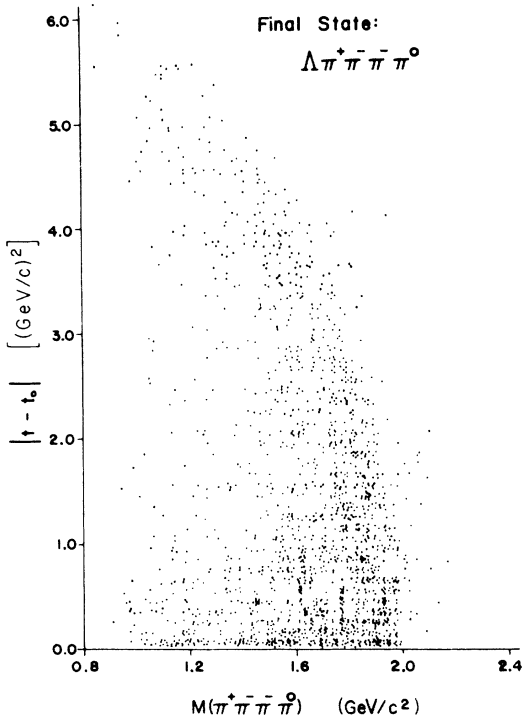

FIG. 22. The Chew-Low plot for the 4π system from $K^-n \to \Lambda\pi^+\pi^-\pi^-\pi^0$.

change of either a strange baryon or a strangeness-2 meson.

E. The Four-Pion Spectrum

Figure 21 shows the 4-pion spectrum of the final state $\Lambda\pi^+\pi^-\pi^-\pi^0$. There is some evidence for an enhancement in the "R" region[21] at about 1.60 GeV/c^2. Baltay *et al.*[22] discuss an isospin-1 object found in the 4π mass spectrum [known as the $\rho(1710)$]. They find a sizable $A_2\pi$ decay mode in addition to a slightly smaller $\omega\pi^-$ decay mode.

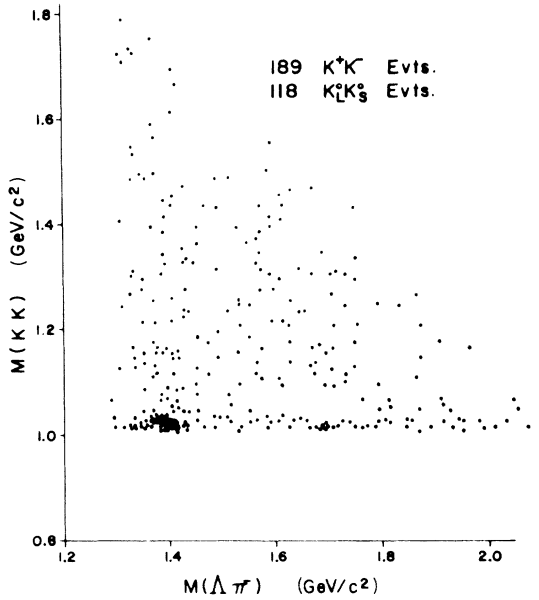

FIG. 24. $\Lambda\pi^-$ mass versus KK mass for $K^-n \to \Lambda\pi^-KK$.

We have searched for an $A_2\pi$ decay mode in our data. The shaded portion of Fig. 21 represents those events for which an appropriate 3π combination may form either a neutral or negative A_2. Choosing events satisfying the condition $1.50 < M(4\pi) < 1.70$ GeV/c^2 and plotting the 3π mass combinations reveals roughly equal A_2^0 and A_2^-.

There is, however, reason to doubt that the object in our data corresponds to the $\rho(1710)$. Although background may be deceiving, our mass appears too low. Secondly, an isospin-1 object should decay to $A_2^0\pi^-$ twice as often as to $A_2^-\pi^0$. Finally there is evidence that our peak for the $A_2\pi$ events may be a kinematic effect. Selecting events having $M(\pi^-\pi^-\pi^0)$ in the "A_2 region" and plotting the 4π combination shows essentially the

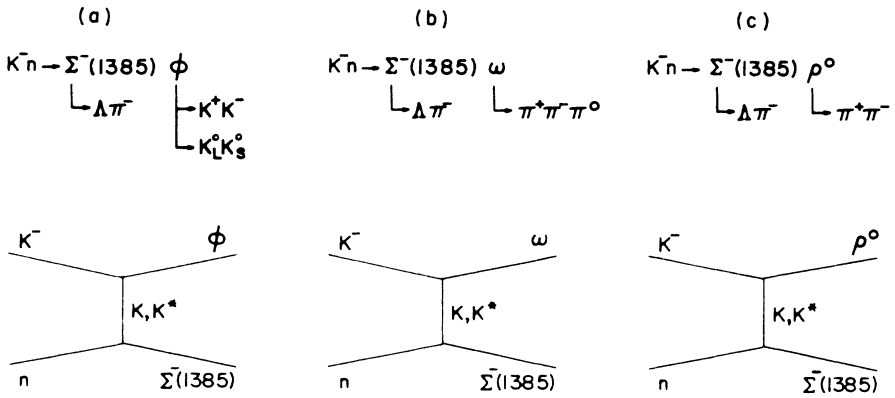

FIG. 23. Diagrams to describe quasi-two-body reactions.

same features as Fig. 21. Furthermore, the Chew-Low plot for this final state is shown in Fig. 22 where the four-momentum transfer is taken from the K^- to the 4π combination. There is no preference for the forward direction.

V. DOUBLE RESONANCE PRODUCTION

This section deals with the study of quasi-two-body reactions of the form

$$K^-n \to \Sigma^-(1385)V^0,$$

where V^0 represents a neutral vector meson. Three vector mesons are considered, the ϕ, ω, and ρ^0 mesons. The production cross sections for these reactions are presented in Table I. All of the reactions are viewed in terms of the diagrams in Fig. 23.

Figures 24–26 show the scatter plots of $M(\Lambda\pi^-)$ versus $M(KK)$, $M(\pi^+\pi^-\pi^0)$, and $M(\pi^+\pi^-)$, respectively. Evidence for the quasi-two-body reactions can be seen in all those graphs.

A. Selection of Quasi-Two-Body Events

The region for double resonance production was defined by mass cuts in the baryon and meson spectra. The ω region is taken as $0.76 < M(\pi^+\pi^-\pi^0) < 0.82$ GeV/c^2, and the ϕ region is taken as $1.0 < M(KK) < 1.04$ GeV/c^2. The $\Sigma(1385)$ and ρ^0 regions are as previously defined, 1.34–1.43 GeV/c^2 and 0.7–0.82 GeV/c^2, respectively.

In addition to the mass cuts, a four-momentum-transfer cutoff at $|t-t_0| = 0.5$ (GeV/c)^2 was imposed in order to reduce background. Using these cuts, we obtain a total of 43, 31, and 14 events for $\Sigma(1385)\phi$, $\Sigma(1385)\omega$, and $\Sigma(1385)\rho^0$, respectively.

B. Angular Distributions

The baryon and meson distributions were investigated separately. All decay angles are given in the Jackson frame. The z direction is defined by the beam in the over-all center-of-mass system. The y direction is the normal to the production plane. Angles θ and φ are the azimuthal and polar angles, respectively, of a decay product in the rest frame of the resonances.

In this coordinate system, the angular distribution for the decay $\Sigma^-(1385) \to \Lambda\pi^-$ has the form[23]

$$W(\theta,\varphi) = \frac{1}{4\pi}[1 - \tfrac{1}{2}(1-4\rho_{11})(3\cos^2\theta - 1) - 2\sqrt{3}\,\mathrm{Re}\rho_{3-1}\sin^2\theta\cos 2\varphi - 2\sqrt{3}\,\mathrm{Re}\rho_{31}\sin 2\theta\cos\varphi].$$

The ρ_{ij} are spin density matrix elements for the decay of a J^P $(\frac{3}{2}^+)$ object into a $(\frac{1}{2}^+)$ and a (0^-) object. At the meson vertex the corresponding distribution is (for the case of three decay products, the normal to the decay plane defines the angles)

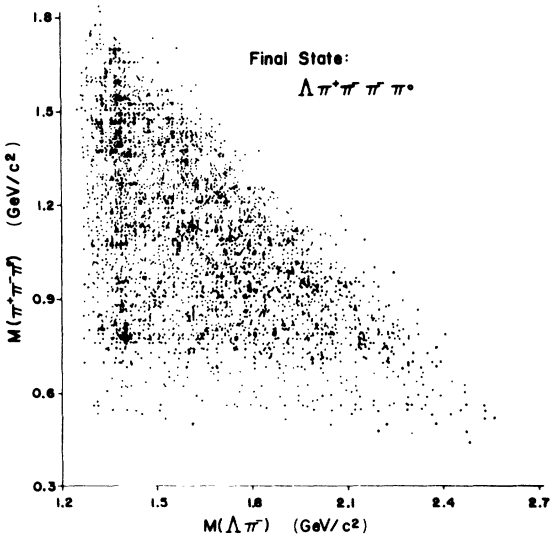

FIG. 25. $\Lambda\pi^-$ mass versus $\pi^+\pi^-\pi^0$ mass for $K^-n \to \Lambda\pi^+\pi^-\pi^-\pi^0$.

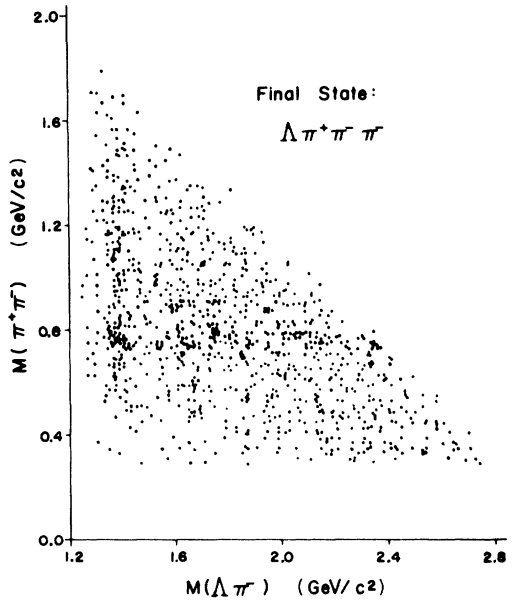

FIG. 26. $\Lambda\pi^-$ mass versus $\pi^+\pi^-$ mass for $K^-n \to \Lambda\pi^+\pi^-\pi^-$.

TABLE V. Density-matrix elements.

	$\Sigma^-(1385)\phi$	$\Sigma^-(1385)\omega$	$\Sigma^-(1385)\rho$
	Meson vertex		
ρ_{00}	0.42± 0.09	0.42± 0.10	0.32± 0.15
$\mathrm{Re}\rho_{10}$	−0.02± 0.04	0.06± 0.06	0.07± 0.05
ρ_{1-1}	0.03± 0.13	−0.16± 0.16	0.13± 0.15
	Baryon vertex		
ρ_{11}	0.38± 0.10	0.49± 0.10	0.38± 0.16
$\mathrm{Re}\rho_{31}$	−0.03± 0.07	−0.12± 0.07	−0.14± 0.12
$\mathrm{Re}\rho_{3-1}$	−0.03± 0.05	−0.06± 0.07	−0.16± 0.09

$$W(\theta,\varphi)=\frac{1}{4\pi}[1-\tfrac{1}{2}(1-3\rho_{00})(3\cos^2\theta-1) - 3\sqrt{2}\,\mathrm{Re}\rho_{10}\sin2\theta\cos\varphi - 3\rho_{1-1}\sin^2\theta\cos2\varphi].$$

The ρ_{ij} are now elements of the spin density matrix for the decay of a $J^P(1^-)$ object into $(0^-)+(0^-)$ or $(0^-)+(0^-)+(0^-)$.

All density-matrix elements were evaluated by the method of moments. Table V contains the calculated density-matrix elements. The principal elements, ρ_{00} at the meson vertex and ρ_{11} at the baryon vertex, are independent of the reaction within errors. Figure 27 displays the angular distributions at the baryon vertex for all three reactions. Smooth curves are drawn using fitted density-matrix elements. Corresponding distributions are shown for the meson vertex in Fig. 28.

C. Quark-Model Predictions

Bialas and Zalewski[24] have derived conditions on spin density-matrix elements using the quark model. They divide their predictions into three classes. Class (A) predictions assume additivity of quark amplitudes without demanding relationships among them. Predictions of class (B) require the additional assumption of equality between two spin-flip quark-quark scattering amplitudes. For class (C) predictions, the remaining two independent spin-flip amplitudes must

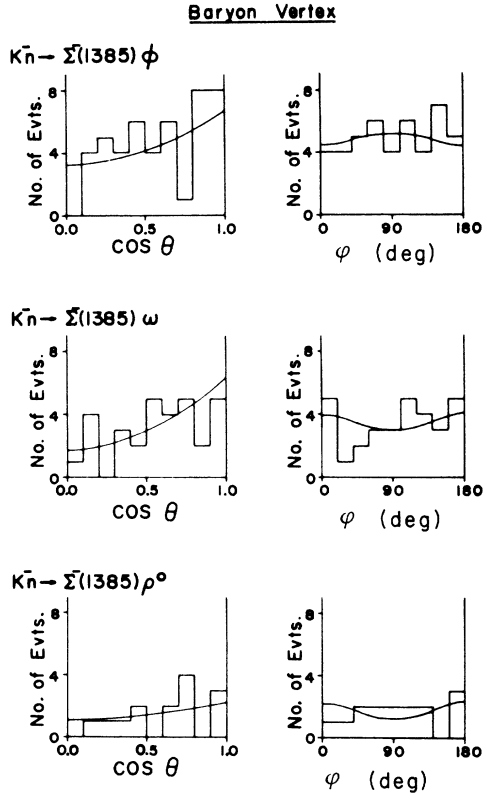

FIG. 27. Angular distributions at baryon vertex. The smooth curves are drawn using the fitted density-matrix elements.

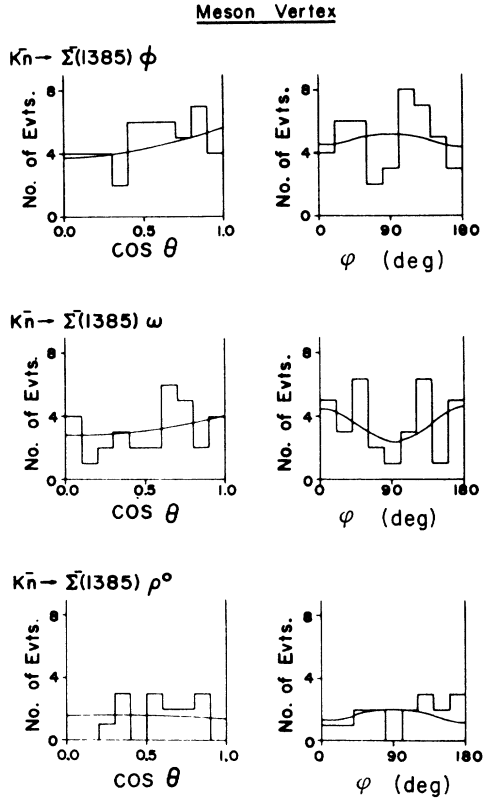

FIG. 28. Angular distributions at meson vertex. The smooth curves are drawn using the fitted density-matrix elements.

also be equal.

Relationships among spin density-matrix elements for the various classes are (meson on left, baryon on right):

$$\text{Class (A)}\quad \tfrac{1}{2}(1-\rho_{00})+\rho_{1-1}=\tfrac{4}{3}(\tfrac{1}{2}-\rho_{11})+\tfrac{4}{3}\sqrt{3}\,\rho_{3-1};$$

$$\text{Class (B)}\quad \tfrac{1}{2}(1-\rho_{00})=\tfrac{4}{3}(\tfrac{1}{2}-\rho_{11}),$$

$$\rho_{1-1}=\tfrac{4}{3}\sqrt{3}\,\rho_{3-1},$$

$$\rho_{10}=\tfrac{2}{3}\sqrt{6}\,\rho_{31};$$

$$\text{Class (C)}\quad \mathrm{Re}\rho_{10}=0,$$

$$\mathrm{Re}\rho_{31}=0.$$

Table VI displays the appropriate quantities for each class for all three reactions. The predictions generally involve complex equations, but only the real parts are tested here. Data involving the ϕ meson are the most reliable since this is the largest and cleanest sample. Predictions for the ρ^0 are included for completeness; uncertain background makes them highly unreliable. Taking the above remark into account, reasonable agreement is found for all three classes with regard to ϕ, ω, and ρ^0 productions, in particular all the ϕ predictions are satisfied within one standard deviation and no equality is wrong by more than 2.2 standard deviations.

Other investigators generally find relations of classes (A) and (B) to be well satisfied, while class (C) relations are badly violated.[25-29]

Using the quark model, Lipkin[30] obtains for the neutral-meson production cross sections:

$$\tfrac{1}{2}\bar{\sigma}(K^-n\to\Sigma^-(1385)\phi)=\bar{\sigma}(K^-n\to\Sigma^-(1385)\omega)$$
$$=\bar{\sigma}(K^-n\to\Sigma^-(1385)\rho^0),$$

where $\bar{\sigma}=\sigma/p_F$, and p_F is the final-state center-of-mass momentum. Our results are

$$\tfrac{1}{2}\bar{\sigma}(\phi):\bar{\sigma}(\omega):\bar{\sigma}(\rho^0)=1.0\pm0.2:0.9\pm0.2:0.5\pm0.3.$$

The relationship between ϕ and ω production is seen to be well satisfied. However, ρ^0 production is about a factor of two lower than expected.

TABLE VI. Density-matrix-element relations.

	Meson vertex	Baryon vertex
Class (A)	$\frac{1}{2}(1-\rho_{00})+\rho_{1-1}$	$\frac{4}{3}(\frac{1}{2}-\rho_{11})+\frac{4}{\sqrt{3}}\rho_{3-1}$
ϕ	0.32 ± 0.14	0.23 ± 0.17
ω	0.13 ± 0.17	−0.13 ± 0.21
ρ^0	0.47 ± 0.17	−0.21 ± 0.24
Class (B)	$\frac{1}{2}(1-\rho_{00})$	$\frac{4}{3}(\frac{1}{2}-\rho_{11})$
ϕ	0.29 ± 0.05	0.16 ± 0.13
ω	0.29 ± 0.05	0.01 ± 0.13
ρ^0	0.34 ± 0.08	0.16 ± 0.13
	ρ_{1-1}	$\frac{4}{\sqrt{3}}\rho_{3-1}$
ϕ	0.03 ± 0.13	0.07 ± 0.11
ω	−0.16 ± 0.16	−0.14 ± 0.16
ρ^0	0.13 ± 0.15	−0.37 ± 0.21
	$\mathrm{Re}\rho_{10}$	$\mathrm{Re}\frac{4}{\sqrt{6}}\rho_{31}$
ϕ	−0.02 ± 0.04	−0.06 ± 0.11
ω	0.06 ± 0.06	−0.20 ± 0.11
ρ^0	0.07 ± 0.05	−0.23 ± 0.20
Class (C)	$\mathrm{Re}\rho_{10}$	$\mathrm{Re}\,\rho_{31}$
ϕ	−0.02 ± 0.04	−0.03 ± 0.07
ω	0.06 ± 0.06	−0.12 ± 0.07
ρ^0	0.07 ± 0.05	−0.14 ± 0.12

Since we consistently find very narrow ρ peaks in this experiment, we may be systematically underestimating the amount of ρ production.

ACKNOWLEDGMENTS

This experiment was initiated under the leadership of the late Professor George W. Tautfest. We would like to express our gratitude to the operating personnel of the bubble chamber and the staff of Argonne National Laboratory, Dr. M. Derrick and Dr. L. Voyvodic in particular. We wish to express our thanks to our programming group, to our scanners and measurers, and to our technical staff.

*Work supported in part by the U. S. Atomic Energy Commission.

†A dissertation based on this work has been submitted to Purdue University in partial fulfillment of the requirements for the Ph.D. degree.

[1]W. L. Yen, A. C. Ammann, D. D. Carmony, A. F. Garfinkel, L. J. Gutay, D. H. Miller, and K. Paler, Nucl. Phys. B35, 317 (1971).

[2]W. L. Yen, A. C. Ammann, D. D. Carmony, R. L. Eisner, A. F. Garfinkel, L. J. Gutay, S. L. Kramer, and D. H. Miller, Phys. Rev. 188, 2011 (1969).

[3]D. D. Carmony, R. L. Eisner, A. C. Ammann, A. F. Garfinkel, L. J. Gutay, D. H. Miller, L. K. Rangan, and W. L. Yen, Phys. Rev. D 2, 30 (1970).

[4]Further details can be found in A. C. Ammann, Ph.D. thesis, Purdue University, 1971 (unpublished).

[5]A. C. Ammann, A. F. Garfinkel, D. D. Carmony, L. J. Gutay, D. H. Miller, and W. L. Yen, Phys. Rev. Letters 24, 327 (1970).

[6]D. J. Crennell, W. C. Delaney, E. Flaminio, U. Kar-

shon, K. W. Lai, W. J. Metzger, J. S. O'Neall, J. M. Scarr, A. M. Thorndike, P. Baumel, R. M. Lea, A. Montwill, and T. G. Schumann, Phys. Rev. Letters 21, 648 (1968).

[7]D. J. Crennell, U. Karshon, K. W. Lai, J. S. O'Neall, J. M. Scarr, P. Baumel, R. M. Lea, T. G. Schumann, and E. M. Urvater, report presented to the Fifth International Conference on Elementary Particles, Lund, Sweden, 1969.

[8]R. J. Abrams, R. L. Cool, G. Giacomelli, T. F. Kycia, B. A. Leontić, K. K. Li, and D. N. Michael, Phys. Rev. Letters 19, 678 (1967).

[9]P. Eberhard, J. H. Friedman, M. Pripstein, and R. R. Ross, Phys. Rev. Letters 22, 200 (1969). See this paper for references to previous analyses of the $\Sigma(1660)$.

[10]R. Armenteros, P. Baillon, C. Bricman, M. Ferro-Luzzi, H. K. Nguyen, V. Pelosi, D. E. Plane, N. Schmitz, E. Burkhardt, H. Filthuth, E. Kluge, H. Oberback, R. R. Ross, R. Barloutaud, P. Granet, J. Meyer, J. L. Narjoux, F. Pierre, J. P. Porte, and J. Prevost, Nucl. Phys. B8, 183 (1968).

[11]Particle Data Group, Phys. Letters 39B, 1 (1972).

[12]A. F. Garfinkel, A. C. Ammann, D. D. Carmony, and W. L. Yen, Phys. Letters 33B, 536 (1970).

[13]G. Goldhaber, J. L. Brown, S. Goldhaber, J. A. Kadyk, B. C. Shen, and G. H. Trilling, Phys. Rev. Letters 12, 336 (1964).

[14]S. U. Chung, O. I. Dahl, L. M. Hardy, R. I. Hess, G. R. Kalbfleisch, J. Kirz, D. H. Miller, and G. A. Smith, Phys. Rev. Letters 12, 621 (1964).

[15]A parametrization of two interfering resonances is given by K. E. Lassila and P. V. Ruuskanen, Phys. Rev. Letters 19, 762 (1967).

[16]G. Chikovani, M. N. Focacci, W. Kienzle, C. Lechanoine, B. Levrat, B. Maglić, M. Martin, P. Schübelin, L. Dubal, M. Fischer, P. Grieder, H. A. Neal, and C. Nef, Phys. Letters 25B, 44 (1967).

[17]D. J. Crennell, U. Karshon, K. W. Lai, J. S. O'Neall, and J. M. Scarr, Phys. Rev. Letters 22, 1327 (1969).

[18]J. K. Kim, Phys. Rev. Letters 19, 1079 (1967).

[19]C. H. Chan and F. T. Meiere, Phys. Rev. Letters 20, 568 (1968).

[20]These expressions can be found in S. U. Chung, O. I. Dahl, J. Kirz, and D. H. Miller, Phys. Rev. 165, 1491 (1968).

[21]J. Seguinot, M. Martin, M. C. Maglić, B. Levrat, F. Lefèbvres, W. Kienzle, M. N. Focacci, L. Dubal, G. Chikovani, C. Bricman, H. R. Blieden, and P. Bareyre, Phys. Letters 19, 712 (1966).

[22]C. Baltay, H. H. Kung, N. Yeh, T. Ferbel, P. F. Slattery, M. Rabin, and H. L. Kraybill, Phys. Rev. Letters 20, 887 (1968).

[23]K. Gottfried and J. D. Jackson, Nuovo Cimento 33, 309 (1964).

[24]A. Bialas and K. Zalewski, Nucl. Phys. B6, 449 (1968); B6, 465 (1968).

[25]B. Haber, A. Shapira, G. Alexander, Y. Eisenberg, E. Hirsch, G. Yekutieli, D. W. Merrill, J. C. Scheuer, L. Monari, P. Serra, S. Focardi, G. Lamidey, and A. Rouge, report submitted to the Fifteenth International Conference on High Energy Physics, Kiev, U.S.S.R., 1970.

[26]B. Haber, A. Shapira, G. Alexander, Y. Eisenberg, E. Hirsch, G. Yekutieli, D. W. Merrill, J. C. Scheuer, L. Monari, P. Serra, S. Focardi, G. Lamidey, and A. Rouge, Nucl. Phys. B17, 289 (1970).

[27]J. H. Friedman and R. R. Ross, Phys. Rev. Letters 22, 152 (1969).

[28]W. Krupac, R. Ammar, H. Yarger, Y. Cho, M. Derrick, D. Johnson, B. Musgrave, T. Wangler, J. Wung, R. Davis, and B. Werner, report submitted to the Fifteenth International Conference on High Energy Physics, Kiev, U.S.S.R., 1970.

[29]F. A. DiBianca, M. B. Einschlag, R. J. Endorf, A. Engler, H. E. Fisk, and R. W. Kraemer, Nucl. Phys. B35, 13 (1971).

[30]H. Lipkin, Nucl. Phys. B7, 321 (1968).